

Detector-induced backaction on the counting statistics of a double quantum dot

Zeng-Zhao Li,¹ Chi-Hang Lam,² Ting Yu,² and J. Q. You¹

¹*Beijing Computational Science Research Center, Beijing 100084, China*

²*Department of Applied Physics, Hong Kong Polytechnic University, Hung Hom, Hong Kong, China*

Full counting statistics of electron transport is of fundamental importance for a deeper understanding of the underlying physical processes in quantum transport in nanoscale devices. The backaction effect from a detector on the nanoscale devices is also essential due to its inevitable presence in experiments. Here we investigate the backaction of a charge detector in the form of a quantum point contact (QPC) on the counting statistics of a biased double quantum dot (DQD). We show that this inevitable QPC-induced backaction can have profound effects on the counting statistics under certain conditions, e.g., changing the shot noise from being sub-Poissonian to super-Poissonian, and changing the skewness from being positive to negative. Also, we show that both Fano factor and skewness can be either enhanced or suppressed by increasing the energy difference between two single-dot levels of the DQD under the detector-induced backaction.

PACS numbers:

Current fluctuations in nanoscale systems provide key insights into the nature of charge transfer beyond what is obtainable from a conductance measurement alone (see, e.g., Refs. 1 and 2 for recent reviews). An in-depth understanding, however, may require us to go beyond the first-order and even the second-order current correlation functions (corresponding to the average current and the shot noise respectively) to study the full counting statistics^{3,4} which yields all zero-frequency correlation functions at once. Real-time detection of the tunneling of individual electrons, an important step towards experimental measurement of the full counting statistics, has recently been achieved in various QD systems⁵⁻⁷. In particular, since its measurement in a single QD for the first time⁸, counting statistics has become an important experimental tool to examine interaction and coherence effects in nanoscale systems under out-of-equilibrium conditions⁹⁻¹³. More recently, counting statistics was applied to characterize correlations in both classical and quantum systems¹⁴.

However, a pronounced effect known as backaction on the counting statistics of electron transport^{2,15} is inevitably introduced during measurements made by even most noninvasive detectors such as a quantum point contact (QPC)¹⁶. Very recently, such backaction has been investigated experimentally in a single QD^{16,17}. In contrast to a single QD, a double quantum dot (DQD)¹⁸ involves coherent coupling between two different dots, and therefore can be used to demonstrate prominent coherent effects¹⁹. The counting statistics for DQDs has been studied theoretically²⁰ and experimentally only for noise properties^{21,22}. In a DQD measured by a QPC, both the current and the shot noise of the QPC have been previously investigated²³⁻²⁶. In addition, for a zero-bias DQD, the effect of charge-detector-induced backaction was studied theoretically²⁷ to explain experimental observations of inelastic electron tunneling²⁸. However, to the best of our knowledge, the impacts of charge-detector-induced backaction on the full counting statistics in these QD systems have not yet been studied.

Here we investigate the counting statistics of electron

transport through a biased DQD under measurement by a charge detector. We demonstrate that this inevitable backaction can indeed have profound effects on the counting statistics under certain conditions for the DQD. In particular, it can change the nature of the shot noise from being sub-Poissonian to super-Poissonian and also change the skewness from being positive to negative. Moreover, we show that when the energy difference between two single-dot levels of the DQD increases, both Fano factor and skewness can be either enhanced or suppressed under the detector-induced backaction. These QPC-backaction-induced effects are expected to be experimentally observable with currently existing technologies. Apart from a deeper understanding of experimental observations, this study may also shed light on how to control these QD systems using the backaction of a charge detector.

Results

We focus on a setup consisting of a lateral DQD, which is coupled to the source and the drain electrodes, and measured by a nearby QPC [see Figure 1(a)]. The lateral DQD is formed by properly tuning the voltages applied to the corresponding gates. Here we consider a Coulomb-blockade regime with strong intradot and interdot Coulomb interactions, so that only one electron is allowed in the DQD system. The states of the DQD are represented by the occupation states $|1\rangle$ and $|2\rangle$, denoting one electron in the left and the right dots, respectively [see Figure 1(b)].

The total Hamiltonian of the whole system can be written as

$$H = H_{\text{DQD}} + H_{\text{leads}} + H_{\text{QPC}} + H_{\text{T}} + H_{\text{det}}, \quad (1)$$

where (we set $\hbar = 1$)

$$H_{\text{DQD}} = \frac{\varepsilon}{2}\sigma_z + \Omega\sigma_x, \quad (2)$$

$$H_{\text{leads}} = \sum_s (\omega_{ls} c_{ls}^\dagger c_{ls} + \omega_{rs} c_{rs}^\dagger c_{rs}), \quad (3)$$

$$H_{\text{QPC}} = \sum_{kq} (\omega_{Sk} c_{Sk}^\dagger c_{Sk} + \omega_{Dq} c_{Dq}^\dagger c_{Dq}), \quad (4)$$

$$H_T = \sum_s [(\Omega_{ls} c_{ls}^\dagger a_1 + \Omega_{rs} \Upsilon_r^\dagger c_{rs}^\dagger a_2) + \text{H.c.}], \quad (5)$$

$$H_{\text{det}} = \sum_{kq} (T - \zeta \sigma_z) (c_{Sk}^\dagger c_{Dq} + c_{Dq}^\dagger c_{Sk}). \quad (6)$$

Here, H_{DQD} , H_{leads} , and H_{QPC} are, respectively, the free Hamiltonians of the DQD, the electrodes coupled to the DQD, and the QPC without the tunneling term. In the DQD Hamiltonian, ε is the energy difference between the two single-dot levels and Ω the interdot tunneling-coupling strength. Also, we define pseudospin operators $\sigma_z \equiv a_2^\dagger a_2 - a_1^\dagger a_1$ and $\sigma_x \equiv a_2^\dagger a_1 + a_1^\dagger a_2$, with a_1 (a_2) being the annihilation operator for an electron staying at the left (right) dot. c_{ls} (c_{rs}) is the annihilation operator for electrons in the source (drain) reservoir, i.e., the left (right) electrode of the DQD, while c_{Sk} (c_{Dq}) is the annihilation operator for electrons in the source (drain) reservoir of the QPC with momentum k (q). H_T gives the tunneling-coupling Hamiltonian between the DQD and the two electrodes where the counting operator Υ_r (Υ_r^\dagger) decreases (increases) the number of electrons that have tunneled into the right electrode (via the barrier between the DQD and the right electrode)²⁹. These counting operators are introduced to keep track of the progress of the tunneling processes by successive electrons. Finally, H_{det} describes tunnelings in the QPC which depends on the electron occupation of the DQD, owing to electrostatic couplings between the DQD and the QPC. We define $T \equiv T_0 - (\zeta_2 + \zeta_1)/2$ and $\zeta \equiv (\zeta_2 - \zeta_1)/2$, so that the transition amplitudes of the QPC, when an extra electron staying at the left and the right dots, equal $T + \zeta$ and $T - \zeta$, respectively³⁰.

A. Counting statistics.

To study the counting statistics of the electron transport through a DQD system, it is essential to know the probability $P(n, t)$ of n electrons having been transported from the DQD to the right electrode during a period of time t . It is related to the cumulant generating function $G(\chi, t)$ defined by²

$$e^{-G(\chi, t)} = \sum_n P(n, t) e^{i\chi n}. \quad (7)$$

We consider the time interval t much longer than the tunneling time of an electron through the DQD system,

so that transient properties (i.e., finite-frequency counting statistics)^{31–33} are insignificant. The derivative of the cumulant generating function with respect to the counting field χ at $\chi = 0$ yields the j -th cumulant, i.e., $C_j = -(-i\partial_\chi)^j G(\chi, t)|_{\chi \rightarrow 0}$, where χ is a field conjugate to n (see, e.g., Ref. 2). These cumulants carry complete information on the counting statistics of the DQD system. For instance, the average current and the shot noise can be expressed as $I = eC_1/t$ and $S = 2e^2 C_2/t$. Thus, the Fano factor F , which is used to characterize the bunching and anti-bunching phenomena in the transport processes, is given by $F = S/2eI = C_2/C_1$. The skewness is defined by $K = C_3/C_1$, which characterizes the asymmetric degree of the distribution of the transported electrons around its mean value.

On the other hand, the probability-distribution function of the number of transported electrons can also be expressed as

$$P(n, t) = \rho_{00}^n(t) + \rho_{gg}^n(t) + \rho_{ee}^n(t), \quad (8)$$

where $\rho_{ij}^n(t)$ ($i, j \in \{0, g, e\}$) denote the reduced density matrix elements of the DQD at a given number n of electrons transported from the DQD to the right electrode in time t . Here 0, g , and e denote the eigenstates $|0\rangle$, $|g\rangle$, and $|e\rangle$ of the DQD, which correspond to no electron staying in the DQD, one electron in the ground state, and one electron in the excited state, respectively [see horizontal solid lines in Figure 1(b)]. From equations (7) and (8), we have

$$\begin{aligned} G(\chi, t) &= -\ln \left\{ \sum_n [\rho_{00}^n(t) + \rho_{gg}^n(t) + \rho_{ee}^n(t)] e^{i\chi n} \right\} \\ &= -\ln [\rho_{00}(\chi, t) + \rho_{gg}(\chi, t) + \rho_{ee}(\chi, t)] \\ &= -\ln \text{Tr}[\rho_{ij}(\chi, t)], \end{aligned} \quad (9)$$

with

$$\rho_{ij}(\chi, t) = \sum_n \rho_{ij}^n(t) e^{i\chi n}. \quad (10)$$

Note that the reduced density matrix elements $\rho_{ij}^n(t)$ in equation (10) satisfy a master equation (see Methods) and $\rho_{ij}(\chi, t)$ are just the Fourier transforms of these matrix elements^{20,22}. Below we manage to obtain the cumulant generating function $G(\chi, t)$ at a long time t .

Based on the master equation of $\rho_{ij}^n(t)$, we can derive the following equation of motion:

$$\frac{\partial \rho}{\partial t} = -\mathcal{M}(\chi) \rho, \quad (11)$$

with

$$\mathcal{M}(\chi) = \begin{pmatrix} \Gamma_L & -\beta^2 \Gamma_R e^{i\chi} & -\alpha^2 \Gamma_R e^{i\chi} & 2\alpha\beta \Gamma_R e^{i\chi} & 0 \\ -\alpha^2 \Gamma_L & \beta^2 \Gamma_R + \gamma_{\text{ex}} & -\gamma_{\text{re}} & -\alpha\beta \Gamma_R - 2\eta\gamma_{\text{de}} & 0 \\ -\beta^2 \Gamma_L & -\gamma_{\text{ex}} & \alpha^2 \Gamma_R + \gamma_{\text{re}} & -\alpha\beta \Gamma_R + 2\eta\gamma_{\text{de}} & 0 \\ -\alpha\beta \Gamma_L & -\frac{1}{2}\alpha\beta \Gamma_R - \eta\gamma_{\text{ex}} & -\frac{1}{2}\alpha\beta \Gamma_R + \eta\gamma_{\text{re}} & \frac{1}{2}\Gamma_R + 2\eta^2\gamma_{\text{de}} & -\Delta \\ 0 & 0 & 0 & \Delta & \frac{1}{2}\Gamma_R + 2\eta^2\gamma_{\text{de}} - \gamma_{\text{ex}} - \gamma_{\text{re}} \end{pmatrix}, \quad (12)$$

where $\varrho \equiv (\rho_{00}(\chi, t), \rho_{gg}(\chi, t), \rho_{ee}(\chi, t), \text{Re}[\rho_{eg}(\chi, t)], \text{Im}[\rho_{eg}(\chi, t)])^T$. Note that $\rho_{0g}(\chi, t)$ and $\rho_{0e}(\chi, t)$ as well as their complex conjugates are decoupled from the reduced density matrix elements given above and therefore are not included. In the matrix $\mathcal{M}(\chi)$, $\alpha = \cos(\theta/2)$, $\beta = \sin(\theta/2)$, and $\eta = \cos\theta$, with $\tan\theta = 2\Omega/\varepsilon$; $\Delta = \sqrt{\varepsilon^2 + 4\Omega^2}$, and $\Gamma_{L(R)} = 2\pi g_{L(R)} \Omega_{lk(rk)}^2$ is the rate of electron tunneling through the barrier between the DQD and the left (right) electrode. Here, g_i ($i = L$, or R) denotes the density of states at the left or the right electrode of the DQD, which is assumed to be constant over the relevant energy range. The QPC-induced excitation rate γ_{ex} , relaxation rate γ_{re} , and dephasing rate γ_{de} are given by

$$\gamma_{\text{ex}} = \lambda [\Theta(eV_{\text{QPC}} - \Delta) + \Theta(-eV_{\text{QPC}} - \Delta)], \quad (13)$$

$$\gamma_{\text{re}} = \lambda [\Theta(eV_{\text{QPC}} + \Delta) + \Theta(-eV_{\text{QPC}} + \Delta)], \quad (14)$$

$$\gamma_{\text{de}} = \lambda [\Theta(eV_{\text{QPC}}) + \Theta(-eV_{\text{QPC}})], \quad (15)$$

where $\Theta(x) = (x + |x|)/2$, and $\lambda = 2\pi g_S g_D \zeta^2$, with g_S (g_D) being the density of states of the source (drain) electrode in the QPC. We also assume g_S and g_D to be constant over the relevant energies³⁴. Let Λ_{\min} be the minimal eigenvalues of $\mathcal{M}(\chi)$ in equation (12). At a long time t , the behavior of $\varrho(\chi, t)$ is dominantly governed by^{36–40}

$$\varrho(\chi, t) = e^{-\Lambda_{\min} t} \varrho(\chi, 0). \quad (16)$$

Therefore, we have $\rho_{ii}(\chi, t) = e^{-\Lambda_{\min} t} \rho_{ii}(\chi, 0)$ at a long time t . Then, it follows from equation (9) that the cumulant generating function at both a small χ and a long time t is given by

$$G(\chi, t) = \Lambda_{\min} t, \quad (17)$$

because $[\rho_{00}(\chi, 0) + \rho_{gg}(\chi, 0) + \rho_{ee}(\chi, 0)]|_{\chi \rightarrow 0} = \sum_i \sum_n \rho_{ii}^n(0) = \sum_i \rho_{ii}(0) = 1$.

Note that the dephasing rate given in equation (15) is proportional to the bias voltage of the QPC, which is consistent with a previous study²³. In addition, our approach is based on the Born-Markov approximation (see Methods), which applies when the rates induced by the backaction from the QPC are weak. With the transition rate of a single electron hopping from one reservoir of the QPC to the other, we can use the Landauer formula to obtain the transition probability²³ and then have $g_S g_D = I_{\text{QPC}} \hbar / (2\pi T^2 e^2 V_{\text{QPC}})$, where I_{QPC} and V_{QPC} are the current and the bias voltage of the QPC with

the densities of states g_S and g_D at the source and the drain reservoirs. Following a recent experiment reported in Ref. 35, we take $I_{\text{QPC}} = 500$ nA and $V_{\text{QPC}} = 0.5$ meV to determine $g_S g_D$. In addition, we choose $\zeta/T = 0.044$ as in Ref. 30, so that the QPC conductance changes by $\sim 1\%$ if the number of electrons in the DQD changes by one³⁵.

B. Detector-induced backaction under resonance condition.

In order to obtain some compact analytical results for the counting statistics, we first consider, for simplicity, the resonance case where energy difference between two single-dot levels is zero (i.e., $\varepsilon = 0$). For instance, the charge current through the DQD is obtained as

$$I = \frac{4e\Gamma_L \Gamma_R \Omega^2}{\Xi}, \quad (18)$$

and shot noise is

$$S = \frac{8e^2 \Gamma_L \Gamma_R \Omega^2 f}{\Xi^3}, \quad (19)$$

where

$$\Xi = \Gamma_L \Gamma_R^2 + 4(2\Gamma_L + \Gamma_R)\Omega^2 - 2\Gamma_L \Gamma_R (\gamma_{\text{ex}} + \gamma_{\text{re}}), \quad (20)$$

$$f = 16\Gamma_R^2 \Omega^4 + \Gamma_L^2 (\Gamma_R^4 - 8\Gamma_R^2 \Omega^2 + 64\Omega^4) + 4\Gamma_L^2 \Gamma_R \times (\gamma_{\text{ex}} + \gamma_{\text{re}}) [-\Gamma_R^2 - 4\Omega^2 + \Gamma_R (\gamma_{\text{ex}} + \gamma_{\text{re}})]. \quad (21)$$

Then, the Fano factor $F \equiv S/2eI$ also follows straightforwardly.

From equations (18)-(21), it is clear that the charge current I , the shot noise S , and hence the Fano factor F depend on the excitation rate γ_{ex} and the relaxation rate γ_{re} induced by the QPC. These reveal the impacts of the backaction from the charge detector. More importantly, because of the nontrivial dependence of both γ_{ex} and γ_{re} on the applied voltage across the QPC [see equations (13) and (14)], the presence of the charge-detector-induced backaction can be experimentally checked. Note that in the case of no backaction, where γ_{ex} and γ_{re} in equations (18) and (19) are equal to zero, our results reduce to the previous results obtained by other approaches^{41,42}. For simplicity, the temperature is here chosen to be zero because it is extremely low in quantum-transport experiments. Other parameters like the interdot coupling

strength Ω and the tunneling rate Γ_L are taken from the experimental data^{21,22}.

The charge current obtained from the cumulant C_1 of the counting statistics is calculated both *with* and *without* backaction, and the results are presented in Figure 2. When the backaction from the charge detector is taken into account, we observe that the current through the DQD is significantly enhanced as shown in Figure 2(a). In particular, when $|eV_{\text{QPC}}| \leq \Delta$, a plateau with a constant current is observed [see, e.g., Figure 2(b)]. This plateau corresponds to a regime in which QPC-induced excitations is suppressed but there is still a constant relaxation rate contributed by the presence of the QPC, as can be interpreted from equations (13) and (14). Physically, a critical energy Δ exists for the QPC-induced excitation of an electron in the DQD and is hence required to change the current^{27,28}. Beyond the regime of constant current, i.e., $|eV_{\text{QPC}}| > \Delta$, it is clearly shown that in the region shown in Figure 2(b) the current increases with the magnitude of the voltage applied across the QPC in a nearly linear manner.

For the Fano factor $F \equiv S/2eI$, our results are given in Figure 3. As shown in Figure 3(a), the nature of the shot noise can be changed from *sub*-Poissonian ($F < 1$) to *super*-Poissonian ($F > 1$), and vice versa, under the QPC-induced backaction. Without backaction, e.g., when the QPC is decoupled to the DQD, the Fano factor is always smaller than one, i.e., *sub*-Poissonian, implying the antibunching of electrons [see the dashed line in Figure 3(b)]. If QPC-induced backaction is considered but with a condition $|eV_{\text{QPC}}| \leq \Delta$, we find a plateau similar to that in the current. As mentioned above, the electron transport in this regime does not involve QPC-induced excitations. Outside this plateau (i.e. $|eV_{\text{QPC}}| > \Delta$), the Fano factor increases with $|V_{\text{QPC}}|$. For a sufficiently large bias, we can get $F = 1$ [see Figures 3(b) and the solid curve in Figure 3(a)], indicating that the electron transport is uncorrelated in time and is described by *Poissonian* statistics. Beyond this large bias, we have $F > 1$. Thus, bunching of electrons in the transport through the DQD occurs, resulting in *super*-Poissonian noise. Physically, the effective tunneling rates for two eigenstate channels are obtained as $\Gamma_R^{(g)} = \beta^2 \Gamma_R + \gamma_{\text{ex}}$ and $\Gamma_R^{(e)} = \alpha^2 \Gamma_R + \gamma_{\text{re}}$ (see Methods). Without backaction, i.e., $\gamma_{\text{re}} = \gamma_{\text{ex}} = 0$, it follows that $\Gamma_R^{(g)} = \Gamma_R^{(e)}$ under the resonance condition (i.e., $\varepsilon = 0$) because of $\alpha = \beta$. This corresponds to *sub*-Poissonian noise (i.e., $F < 1$). For example, $F \approx 0.39$ for the dashed line in Figure 3(b). When the detector-induced backaction is included, i.e., $\gamma_{\text{re}}, \gamma_{\text{ex}} \neq 0$, the effective tunneling rates become unequal (i.e., $\Gamma_R^{(e)} \neq \Gamma_R^{(g)}$) even if $\alpha = \beta$ under the resonance condition. This increases F but F is still smaller than 1 for small values of $|eV_{\text{QPC}}|$. However, when $|eV_{\text{QPC}}|$ further increases, it enhances γ_{re} and γ_{ex} [see equations (13) and (14)], i.e., the relaxation and the excitation. This makes the two effective tunneling rates more asymmetric, yielding $F > 1$ (i.e., *super*-Poissonian noise) at large values of $|eV_{\text{QPC}}|$. Therefore, the change of shot noise from being

sub-Poissonian to *super*-Poissonian is due to the effect of dynamical blocked channels^{43–45} induced by the QPC backaction.

We also numerically calculate the skewness $K = C_3/C_1$ (see Figure 4). As demonstrated in Figure 4(a), the skewness can be changed from being positive ($K > 0$) to negative ($K < 0$), and vice versa, under the QPC-induced backaction. Here $K = 0$ corresponds to a symmetric Gaussian distribution of electron tunneling, where the tunneling of the larger number of electrons in a given time duration occurs with the same probability as the tunneling of the smaller number of electrons, with respect to a mean value. For $K > 0$ ($K < 0$), the distribution of electron tunneling becomes asymmetric with the tunneling of the larger number of electrons in a given duration occurring with a higher (lower) probability. Without backaction, the skewness is always positive [see the dashed line in Figure 4(b)]. When QPC-induced backaction is included but with $|eV_{\text{QPC}}| \leq \Delta$, a plateau similar to that in either current or Fano factor appears. In this region, QPC-induced excitations are not involved in the electron transport. Outside this region (i.e., $|eV_{\text{QPC}}| > \Delta$), the skewness can be either positive or negative, depending on the values of Γ_R and $|eV_{\text{QPC}}|$ [see Figure 4(b) and the regions surrounded by solid curves in Figure 4(a)]. This indicates that the distribution of transported electrons can deviate from the Gaussian in an opposite way.

C. Detector-induced backaction under off-resonance condition.

Note that the QPC-induced dephasing is not discussed above. This is because such dephasing with a rate $\gamma_{\text{de}} (= \lambda|eV_{\text{QPC}}|)$ does not induce any transitions between different states of the DQD. However, it is known that dephasing produces broadening of the energy levels of the DQD²³, and then can affect the current. Indeed, in this case, the resonance condition (i.e., $\varepsilon = 0$) may be violated. Below we numerically study the backaction effect under the off-resonance condition (i.e., $\varepsilon \neq 0$) because analytical results cannot be derived in this more general case.

To investigate the effect of the energy difference ε on the detector-induced backaction, we calculate the current, the shot noise, the Fano factor, and the skewness using the same parameters as in Figures 2(b) and 3(b). In Figure 5(a), the dotted curve shows the behavior of the current under the resonance condition (i.e., $\varepsilon = 0$). When the energy difference ε increases, the current decreases [see the dashed and solid curves in Figure 5(a)]. Moreover, within the region $|eV_{\text{QPC}}| < \Delta$, the current decreases with increasing $|eV_{\text{QPC}}|$ under the off-resonance condition (i.e., $\varepsilon \neq 0$). Outside the region, i.e., $|eV_{\text{QPC}}| \geq \Delta$, the current varies more nonlinearly with the voltage V_{QPC} , as compared with the current under $\varepsilon = 0$. Physically, the increase of ε , e.g., from $\varepsilon = 0$

to 0.2 meV, makes the electron tunneling between the two dots more off-resonant, so the current through them decreases²³. In addition, the QPC-induced dephasing can yield the broadening of the energy levels at a given nonzero ε , which can further reduce the current²³. The effect of dephasing is contrary to the effects of excitation and relaxation which increase the current [see equation (18)]. As a result, these two opposite effects compete in the electron-tunneling processes at a given nonzero ε . Within the region $|eV_{\text{QPC}}| < \Delta$, the dephasing effect dominates, leading to a decreasing current with the increase of $|eV_{\text{QPC}}|$. Outside this region, i.e., $|eV_{\text{QPC}}| > \Delta$, both relaxation and excitation processes play an important role, so the current increases with $|eV_{\text{QPC}}|$.

The results of the shot noise (i.e., $S/2e$) are shown in Figure 5(b). The shot noise decreases with the increase of the energy difference ε . At a given nonzero ε , the shot noise decreases with increasing $|eV_{\text{QPC}}|$ within the region $|eV_{\text{QPC}}| < \Delta$. Outside this region, i.e., $|eV_{\text{QPC}}| > \Delta$, the shot noise increases with $|eV_{\text{QPC}}|$. These behaviors are similar to those of the current. From both current and shot noise, the Fano factor is straightforwardly obtained, as shown in Figure 5(c). When $|eV_{\text{QPC}}|$ is small, the Fano factor increases with the energy difference ε . However, for large values of $|eV_{\text{QPC}}|$, Fano factor is suppressed. Moreover, the Fano factor first decreases and then increases with $|eV_{\text{QPC}}|$ at a given nonzero ε . These behaviors can be deduced from the current in Figure 5(a) and the shot noise in Figure 5(b) since $F = S/2eI$. Physically, the off-resonance electron tunneling between two dots is enhanced when increasing ε . This off-resonance makes the two eigenstate channels more asymmetric (i.e., $\Gamma_R^{(e)} \neq \Gamma_R^{(g)}$) around the region $|eV_{\text{QPC}}| < \Delta$, and then the Fano factor increases due to dynamical blockaded channels^{43–45}. For large values of $|eV_{\text{QPC}}|$ where backaction becomes strong, the decrease of the Fano factor with increasing ε may be due to the QPC-induced backaction.

The results of the skewness are shown in Figure 5(d). For small values of $|eV_{\text{QPC}}|$, the skewness increases with ε . However, the skewness is suppressed when $|eV_{\text{QPC}}|$ becomes large. Also, the skewness first decreases and then increases with $|eV_{\text{QPC}}|$ at a given nonzero ε . These behaviors are similar to those of the Fano factor, which also indicate that the off-resonance electron tunneling dominates for small values of $|eV_{\text{QPC}}|$ and the QPC-induced backaction plays an important role for large values of $|eV_{\text{QPC}}|$.

Discussion

Note that in the strong Coulomb-blockade regime, we only need to consider the lowest two energy levels of the DQD. In this aspect, it is similar to the single two-level dot in Ref. 45. However, the DQD are different from the single two-level dot in other aspects. For instance, the DQD provides more controllabilities than a single quantum dot. It can be tuned by not only the two single-

dot levels of the DQD but also the interdot tunneling strength via gate voltages. However, in a single quantum dot, only the level spacing can be tuned by the trap potential of the dot. Also, the electron transport through a single quantum dot only involves the tunneling rates Γ_L and Γ_R , while the electron transport through the DQD involves the effective tunneling rates of the two eigenstate channels, i.e., $\Gamma_L^{(g)} = \alpha^2\Gamma_L$, $\Gamma_L^{(e)} = \beta^2\Gamma_L$, $\Gamma_R^{(g)} = \beta^2\Gamma_R + \gamma_{\text{ex}}$ and $\Gamma_R^{(e)} = \alpha^2\Gamma_R + \gamma_{\text{re}}$ (see Methods), which depend on the energy difference ε of the two single-dot levels and the tunneling strength Ω between these two levels. As seen in Methods, both α and β are functions of ε and Ω . Moreover, in our considered setup, the QPC can induce excitation and relaxation as well as dephasing on the electron that tunnels through the DQD [see the interaction Hamiltonian in the eigenstate basis, i.e., equations (23), (25) and (26) in Methods]. This is also different from a single quantum dot because the QPC can only induce dephasing on the electron that tunnels through this single dot⁸.

In summary, we have studied the unavoidable detector-induced backaction on the counting statistics of a biased DQD. We find that this backaction has profound effects on the counting statistics, e.g., changing the shot noise from being sub-Poissonian regime to super-Poissonian, and changing the skewness from being positive to negative. We also show that when the energy difference between two single-dot levels of the DQD increases, both Fano factor and skewness can be either enhanced or suppressed under the detector-induced backaction. These backaction effects can be experimentally examined by using the current technologies. Also, our results contribute to possible fine manipulation of quantum transport processes using the backaction of a charge detector.

Methods

Quantum dynamics of the DQD. We derive a master equation to describe the quantum dynamics of the DQD²⁷, which is used to calculate the counting statistics. In the eigenstate basis, the DQD Hamiltonian can be written as

$$H_{\text{DQD}} = \frac{\Delta}{2}(|e\rangle\langle e| - |g\rangle\langle g|), \quad (22)$$

where $\Delta = \sqrt{\varepsilon^2 + 4\Omega^2}$ is the energy splitting of the two eigenstates of the DQD given by $|g\rangle = \alpha|1\rangle - \beta|2\rangle$, and $|e\rangle = \beta|1\rangle + \alpha|2\rangle$, with $\alpha = \cos(\theta/2)$, $\beta = \sin(\theta/2)$, and $\tan\theta = 2\Omega/\varepsilon$. In the interaction picture with the unperturbed Hamiltonian $H_0 \equiv H_{\text{DQD}} + H_{\text{leads}} + H_{\text{QPC}}$, the interaction Hamiltonian $H_I \equiv H_T + H_{\text{det}}$ can be written as

$$H_{\text{det}} = X(t)Y(t), \quad (23)$$

$$H_T(t) = \sum_s [c_{ls}^\dagger (\alpha a_g e^{-i\Delta t/2} + \beta a_e e^{i\Delta t/2}) e^{i\omega_{ls}t} + \Upsilon_r^\dagger c_{rs}^\dagger \times (\alpha a_e e^{i\Delta t/2} - \beta a_g e^{-i\Delta t/2}) e^{i\omega_{rs}t} + \text{H.c.}], \quad (24)$$

where

$$X(t) = \sum_{n=1}^3 U_n e^{i\omega_n t}, \quad (25)$$

$$Y(t) = \sum_{kq} V_{kq}^\dagger(t) + V_{kq}(t), \quad (26)$$

and $U_1 = \zeta|e\rangle\langle g|$, $U_2 = \zeta|g\rangle\langle e|$, $U_3 = T - \zeta \cos \theta_{\mathcal{Q}_z}$, $\omega_1 = -\omega_2 = \Delta$, $\omega_3 = 0$, $V_{kq}(t) = c_{Dq}^\dagger c_{Sk} e^{-i(\omega_{Sk} - \omega_{Dk})t}$. a_e and a_g are annihilation operators for eigenstates $|e\rangle$ and $|g\rangle$, respectively.

Applying the Born-Markov approximation and tracing over the degrees of freedom of the QPC, the quantum dynamics of the DQD system in the Schrödinger picture is governed by the master equation,

$$\dot{\rho}(t) = -i[H_{\text{DQD}}, \rho(t)] + \mathcal{L}_d \rho(t) + \mathcal{L}_T \rho(t), \quad (27)$$

with

$$\mathcal{L}_d \rho(t) = \sum_{i,j=1, i \neq j}^3 \{ \mathcal{D}[U_i] \rho(t) + \mathcal{D}[U_i, U_j] \rho(t) \} \times \lambda [\Theta(eV_{\text{QPC}} - \omega_i) + \Theta(-eV_{\text{QPC}} - \omega_i)] \quad (28)$$

$$\begin{aligned} \mathcal{L}_T \rho(t) = & \alpha^2 \Gamma_L \mathcal{D}[a_g^\dagger] \rho(t) + \beta^2 \Gamma_L \mathcal{D}[a_e^\dagger] \rho(t) \\ & + \alpha^2 \Gamma_R \mathcal{D}[a_e \Upsilon^\dagger] \rho(t) + \beta^2 \Gamma_R \mathcal{D}[a_g \Upsilon^\dagger] \rho(t) \\ & + \alpha \beta \Gamma_L \{ [a_e^\dagger, \rho(t) a_g] + [a_g^\dagger \rho(t), a_e] \\ & + [a_g^\dagger, \rho(t) a_e] + [a_e^\dagger \rho(t), a_g] \} \\ & - \alpha \beta \Gamma_R \{ [a_e \Upsilon^\dagger, \rho(t) a_g^\dagger \Upsilon] + [a_g \Upsilon^\dagger \rho(t), a_e^\dagger \Upsilon] \\ & + [a_g^\dagger \Upsilon^\dagger, \rho(t) a_e^\dagger \Upsilon] + [a_e \Upsilon^\dagger \rho(t), a_g^\dagger \Upsilon] \}. \quad (29) \end{aligned}$$

Here, $\rho(t)$ is the reduced density matrix of the DQD system. The theta functions $\Theta(\pm eV_{\text{QPC}} - \omega_i)$ appear when tracing over the degrees of freedom of the QPC, i.e., $\int_{-\infty}^{\mu_L} \int_{\mu_R}^{+\infty} g_S g_D d\omega_k d\omega_q \int_0^{+\infty} d\tau e^{i\omega\tau} e^{-i(\omega_k - \omega_q)\tau} \langle c_{Sk}^\dagger c_{Dq} c_{Dq}^\dagger c_{Sk} \rangle = \pi g_S g_D \Theta(eV_{\text{QPC}} - \omega)$, and $\int_{\mu_L}^{+\infty} \int_{-\infty}^{\mu_R} g_S g_D d\omega_k d\omega_q \int_0^{+\infty} d\tau e^{i\omega\tau} e^{i(\omega_k - \omega_q)\tau} \langle c_{Dq}^\dagger c_{Sk} c_{Sk}^\dagger c_{Dq} \rangle = \pi g_S g_D \Theta(-eV_{\text{QPC}} - \omega)$, with $eV_{\text{QPC}} = \mu_L - \mu_R$, where μ_L and μ_R are the chemical potentials of the source and drain electrodes of the QPC. For $\omega > 0$, the QPC-induced excitation occurs when $|eV_{\text{QPC}}| > \omega$ [see equation (13)]. For $\omega < 0$ or $\omega = 0$, the QPC-induced excitation or dephasing occurs, respectively [see equations (14) and (15)]. The superoperator \mathcal{D} , acting on any single or double operator, is defined as

$$\mathcal{D}[A] \rho \equiv A \rho A^\dagger - \frac{1}{2} A^\dagger A \rho - \frac{1}{2} \rho A^\dagger A, \quad (30)$$

$$\mathcal{D}[A, B] \rho \equiv \frac{1}{2} (A \rho B^\dagger + B \rho A^\dagger - B^\dagger A \rho - \rho A^\dagger B). \quad (31)$$

From equation (27) and the relations

$$\langle n | \Upsilon_r^\dagger \rho \Upsilon_r | n \rangle = \rho^{(n-1)}, \quad \langle n | \Upsilon_r \rho \Upsilon_r^\dagger | n \rangle = \rho^{(n+1)}, \quad (32)$$

$$\langle n | \Upsilon_r^\dagger \Upsilon_r \rho | n \rangle = \rho^{(n)}, \quad \langle n | \Upsilon_r \Upsilon_r^\dagger \rho | n \rangle = \rho^{(n)}, \quad (33)$$

where n is the number of electrons that have tunneled to the right electrode of the DQD, we obtain the n -resolved equation of motion for each reduced density matrix element:

$$\begin{aligned} \dot{\rho}_{00}^{(n)} = & -\Gamma_L \rho_{00}^{(n)} + \beta^2 \Gamma_R \rho_{gg}^{(n-1)} + \alpha^2 \Gamma_R \rho_{ee}^{(n-1)} \\ & - \alpha \beta \Gamma_R (\rho_{eg}^{(n-1)} + \rho_{ge}^{(n-1)}), \quad (34) \end{aligned}$$

$$\begin{aligned} \dot{\rho}_{gg}^{(n)} = & \alpha^2 \Gamma_L \rho_{00}^{(n)} - (\beta^2 \Gamma_R + \gamma_{\text{ex}}) \rho_{gg}^{(n)} + \gamma_{\text{re}} \rho_{ee}^{(n)} \\ & + (\frac{1}{2} \alpha \beta \Gamma_R + \eta \gamma_{\text{de}}) (\rho_{eg}^{(n)} + \rho_{ge}^{(n)}), \quad (35) \end{aligned}$$

$$\begin{aligned} \dot{\rho}_{ee}^{(n)} = & \beta^2 \Gamma_L \rho_{00}^{(n)} + \gamma_{\text{ex}} \rho_{gg}^{(n)} - (\alpha^2 \Gamma_R + \gamma_{\text{re}}) \rho_{ee}^{(n)} \\ & + (\frac{1}{2} \alpha \beta \Gamma_R - \eta \gamma_{\text{de}}) (\rho_{eg}^{(n)} + \rho_{ge}^{(n)}), \quad (36) \end{aligned}$$

$$\begin{aligned} \dot{\rho}_{eg}^{(n)} = & -i \Delta \rho_{eg}^{(n)} + \alpha \beta \Gamma_L \rho_{00}^{(n)} + (\frac{1}{2} \alpha \beta \Gamma_R + \eta \gamma_{\text{ex}}) \rho_{gg}^{(n)} \\ & + (\frac{1}{2} \alpha \beta \Gamma_R - \eta \gamma_{\text{re}}) \rho_{ee}^{(n)} - (\frac{1}{2} \Gamma_R + 2\eta^2 \gamma_{\text{de}}) \rho_{eg}^{(n)} \\ & - \frac{1}{2} (\gamma_{\text{ex}} + \gamma_{\text{re}}) (\rho_{eg}^{(n)} - \rho_{ge}^{(n)}). \quad (37) \end{aligned}$$

In particular, we obtain the tunneling rates for two eigenstate channels $\Gamma_L^{(g)} = \alpha^2 \Gamma_L$, $\Gamma_L^{(e)} = \beta^2 \Gamma_L$, $\Gamma_R^{(g)} = \beta^2 \Gamma_R + \gamma_{\text{ex}}$, and $\Gamma_R^{(e)} = \alpha^2 \Gamma_R + \gamma_{\text{re}}$.

- ¹ Blanter, Y. & Büttiker, M. Shot noise in mesoscopic conductors. *Phys. Rep.* **336**, 1-166 (2000).
- ² Nazarov, Y. V. *Quantum Noise in Mesoscopic Physics* (Kluwer, Dordrecht, 2003).
- ³ Levitov, L. S. & Lesovik, G. B. Charge distribution in quantum shot noise. *JETP Lett.* **58**, 230-235 (1993).
- ⁴ Levitov, L. S., Lee, H. W. & Lesovik, G. B. Electron counting statistics and coherent states of electric current. *J. Math. Phys.* **37**, 4845-4866 (1996).
- ⁵ Lu, W., Ji, Z., Pfeiffer, L., West, K. W. & Rimberg, A. J. Real-time detection of electron tunnelling in a quantum dot. *Nature (London)* **423**, 422-425 (2003).
- ⁶ Fujisawa, T., Hayashi, T., Hirayama, Y., Cheong, H. D. & Jeong, Y. H. Electron counting of single-electron tunneling current. *Appl. Phys. Lett.* **84**, 2343-2345 (2004).
- ⁷ Bylander, J., Duty, T. & Delsing, P. Current measurement by real-time counting of single electrons. *Nature (London)* **434**, 361-364 (2005).
- ⁸ Gustavsson, S. *et al.* Counting statistics of single electron transport in a quantum dot. *Phys. Rev. Lett.* **96**, 076605 (2006).
- ⁹ Flindt, C. *et al.* Universal oscillations in counting statistics. *Proc. Natl. Acad. Sci. USA* **106**, 10116-10119 (2009).
- ¹⁰ Gabelli, J. & Reulet, B. Full counting statistics of avalanche transport: An experiment. *Phys. Rev. B* **80**, 161203(R) (2009).
- ¹¹ Fricke, C., Hohls, F., Sethubalasubramanian, N., Fricke, L. & Haug, R. J. High-order cumulants in the counting statistics of asymmetric quantum dots. *Appl. Phys. Lett.* **96**, 202103 (2010).
- ¹² Choi, T., Ihn, T., Schön, S. & Ensslin, K. Counting statistics in an InAs nanowire quantum dot with a vertically coupled charge detector. *Appl. Phys. Lett.* **100**, 072110 (2012).
- ¹³ Ubbelohde, N., Fricke, C., Flindt, C., Hohls, F. & Haug, R. J. Measurement of finite-frequency current statistics in a single electron transistor. *Nature Communications* **3**, 612 (2012).
- ¹⁴ Ivanov, D. A. & Abanov, A. G. Characterizing correlations with full counting statistics: Classical Ising and quantum XY spin chains. *Phys. Rev. E* **87**, 022114 (2013).
- ¹⁵ Nazarov, Y. V. & Kindermann, M. Full counting statistics of a general quantum mechanical variable. *Eur. Phys. J. B* **35**, 413-420 (2003).
- ¹⁶ Sukhorukov, E. V. *et al.*, Conditional statistics of electron transport in interacting nanoscale conductors. *Nat. Phys.* **3**, 243-247 (2007).
- ¹⁷ Li, H. O. *et al.* Back-action-induced non-equilibrium effect in electron charge counting statistics. *Appl. Phys. Lett.* **100**, 092112 (2012).
- ¹⁸ van der Wiel, W. G. *et al.* Electron transport through double quantum dots. *Rev. Mod. Phys.* **75**, 1-22 (2002).
- ¹⁹ Lambert, N., Emary, C., Chen, Y. N. & Nori, F. Distinguishing quantum and classical transport through nanostructures. *Phys. Rev. Lett.* **105**, 176801 (2010).
- ²⁰ Kießich, G., Samuelsson, P., Wacker, A. & Schöll, E. Counting statistics and decoherence in coupled quantum dots. *Phys. Rev. B* **73**, 033312 (2006).
- ²¹ Barthold, P., Hohls, F., Maire, N., Pierz, K. & Haug, R. J. Enhanced shot noise in tunneling through a stack of coupled quantum dots. *Phys. Rev. Lett.* **96**, 246804 (2006).
- ²² Kießich, G., Schöll, E., Brandes, T., Hohls, F. & Haug, R. J. Noise enhancement due to quantum coherence in coupled quantum dots. *Phys. Rev. Lett.* **99**, 206602 (2007).
- ²³ Gurvitz, S. A. Measurements with a noninvasive detector and dephasing mechanism. *Phys. Rev. B* **56**, 15215-15223 (1997).
- ²⁴ Korotkov, A. N. Selective quantum evolution of a qubit state due to continuous measurement. *Phys. Rev. B* **63**, 115403 (2001).
- ²⁵ Ruskov, R. & Korotkov, A. N. Spectrum of qubit oscillations from generalized Bloch equations. *Phys. Rev. B* **67**, 075303 (2003).
- ²⁶ Young, C. E. & Clerk, A. A. Inelastic backaction due to quantum point contact charge fluctuations. *Phys. Rev. Lett.* **104**, 186803 (2010).
- ²⁷ Ouyang, S. H., Lam, C. H. & You, J. Q. Backaction of a charge detector on a double quantum dot. *Phys. Rev. B* **81**, 075301 (2010).
- ²⁸ Gustavsson, S. *et al.* Frequency-selective single-photon detection using a double quantum dot. *Phys. Rev. Lett.* **99**, 206804 (2007).
- ²⁹ Doiron, C. B., Trauzettel, B. & Bruder, C. Improved position measurement of nanoelectromechanical systems using cross correlations. *Phys. Rev. B* **76**, 195312 (2007).
- ³⁰ Li, Z. Z., Ouyang, S. H., Lam, C. H. & You, J. Q. Probing the quantum behavior of a nanomechanical resonator coupled to a double quantum dot. *Phys. Rev. B* **85**, 235420 (2012).
- ³¹ Emary, C., Marcos, D., Aguado, R. & Brandes, T. Frequency-dependent counting statistics in interacting nanoscale conductors. *Phys. Rev. B* **76**, 161404(R) (2007).
- ³² Marcos, D., Emary, C., Brandes, T. & Aguado, R. Finite-frequency counting statistics of electron transport: Markovian theory. *New J. Phys.* **12**, 123009 (2010).
- ³³ Albert, M., Flindt, C. & Büttiker, M. Distributions of waiting times of dynamic single-electron emitters. *Phys. Rev. Lett.* **107**, 086805 (2011).
- ³⁴ Stace, T. M. & Barrett, S. D. Continuous quantum measurement: Inelastic tunneling and lack of current oscillations. *Phys. Rev. Lett.* **92**, 136802 (2004).
- ³⁵ Vandersypen, L. M. K. *et al.* Real-time detection of single-electron tunneling using a quantum point contact. *Appl. Phys. Lett.* **85**, 4394-4396 (2004).
- ³⁶ Bagrets, D. A. & Nazarov, Y. V. Full counting statistics of charge transfer in Coulomb blockade systems. *Phys. Rev. B* **67**, 085316 (2003).
- ³⁷ Flindt, C., Novotný, T. & Jauho, A. P. Full counting statistics of nano-electromechanical systems. *Europhys. Lett.* **69**, 475-481 (2005).
- ³⁸ Flindt, C., Novotný, T., Braggio, A., Sassetti, M. & Jauho, A. P. Counting statistics of non-Markovian quantum stochastic processes. *Phys. Rev. Lett.* **100**, 150601 (2008).
- ³⁹ Braggio, A., Flindt, C. & Novotný, T. The influence of charge detection on counting statistics. *J. Stat. Mech.* P01048 (2009).
- ⁴⁰ Luo, J. Y. *et al.* Full counting statistics of level renormalization in electron transport through double quantum dots. *J. Phys.: Condens. Matter* **23**, 145301 (2011).
- ⁴¹ Gurvitz, S. A. & Prager, Y. S. Microscopic derivation of rate equations for quantum transport. *Phys. Rev. B* **53**,

- 15932-15943 (1996).
- ⁴² Nazarov, Y. V. & Struben, J. J. R. Universal excess noise in resonant tunneling via strongly localized states. *Phys. Rev. B* **53**, 15466-15468 (1996).
- ⁴³ Cottet, A., Belzig, W. & Bruder, C. Positive cross correlations in a three-terminal quantum dot with ferromagnetic contacts. *Phys. Rev. Lett.* **92**, 206801 (2004).
- ⁴⁴ Cottet, A. & Belzig, W. Dynamical spin-blockade in a quantum dot with paramagnetic leads. *Europhys. Lett.* **66**, 405-411 (2004).
- ⁴⁵ Belzig, W. Full counting statistics of super-Poissonian shot noise in multilevel quantum dots. *Phys. Rev. B* **71**, 161301 (2005).

Acknowledgements

This work is supported by the National Basic Research Program of China Grant No. 2009CB929302, the National Natural Science Foundation of China Grant No. 91121015, NSF PHY-0925174, and the China Postdoctoral Science Foundation Grant No. 2012M520146.

Author Contributions

Z.Z.L. performed the calculations under the guidance of J.Q.Y., and both C.H.L. and T.Y. also participated in the discussions. All authors contributed to the interpretation of the work and the writing of the manuscript.

Figure 1 The coupled QDQ-QPC system. (a) Schematic diagram of a DQD coupled to two electrodes (S and D) via tunneling barriers. A QPC used for measuring the DQD electron states yields backaction on the DQD. (b) Electronic transition between two eigenstates $|g\rangle$ and $|e\rangle$ of the DQD (with a transition energy Δ) can be induced by the charge detector QPC. The energy difference ε between the two single-dot levels (dashed lines) can be varied by tuning the gate voltages.

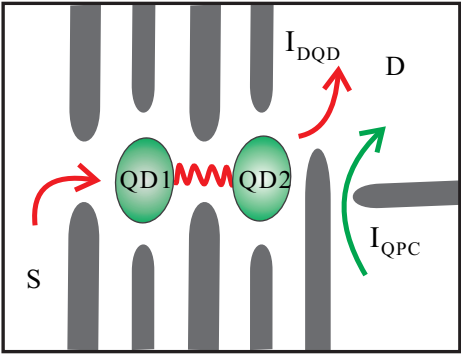
Figure 2 Current under QPC-induced backaction at the resonance condition. (a) Current I versus the QPC bias energy eV_{QPC} and the tunneling rate Γ_R . (b) Current I versus the QPC bias energy eV_{QPC} for a given tunneling rate $\Gamma_R = 0.15$ meV. We use typical experimental parameters $\Omega = 0.1$ meV and $\Gamma_L = 0.05$ meV from Refs. 21 and 22.

Figure 3 Fano factor under QPC-induced backaction at the resonance condition. (a) Fano factor F versus QPC bias energy eV_{QPC} and the tunneling rate Γ_R . (b) Fano factor versus the bias energy eV_{QPC} for a given tunneling rate $\Gamma_R = 0.15$ meV. Other parameters are the same as in Figure 2.

Figure 4 Skewness under QPC-induced backaction at the resonance condition. (a) Skewness K versus QPC bias energy eV_{QPC} and the tunneling rate Γ_R . (b) Skewness versus the bias energy eV_{QPC} for a given tunneling rate $\Gamma_R = 0.25$ meV. Other parameters are the same as in Figure 2.

Figure 5 Current, shot noise, Fano factor and skewness under QPC-induced backaction at the off-resonance condition. (a) Current I , (b) shot noise, (c) Fano factor F , and (d) skewness K versus the QPC bias energy eV_{QPC} for different values of the energy difference ε between two single-dot levels of the DQD. We use a typical experimental parameter $\Gamma_R = 0.15$ meV. Other parameters are the same as in Figure 2.

(a)



(b)

